**Supplementary Table S1** Data collection and phasing statistics.

| | Native | Se-Met | | |
|---|---|---|---|---|
| Data set | | peak | edge | remote |
| Wavelength (Å) | 0.9950 | 0.9793 | 0.9795 | 0.9641 |
| Resolution (Å) | 50-1.65 | 50-1.90 | 50-1.90 | 50-1.90 |
| Observed reflections | 281458 | 301333 | 295418 | 289492 |
| Unique reflections | 70306 | 47655 | 47429 | 47380 |
| Completeness (%)[a] | 97.3 (85.9) | 99.5 (97.3) | 99.5 (99.8) | 99.4 (99.6) |
| $I/\sigma$ | 30.5(1.81) | 34.9(3.62) | 38.7(5.36) | 37.0(4.95) |
| $R_{sym}$ (%)[a,b] | 8.2 (55.4) | 8.8 (44.6) | 11.1 (42.9) | 11.3 (44.6) |
| Phasing | | | | |
| Phasing Power[c] (anomalous) | | 0.8 | 0.4 | 0.4 |
| Phasing Power[c] (dispersive) | | | | |
| peak vs edge | | 0.2 | | |
| peak vs remote | | 0.4 | | |
| edge vs remote | | 0.7 | | |
| Mean Figure of Merit | | 0.50 | | |

[a]Values in parentheses refer to data in the highest resolution shell, 1.71-1.65 Å for the native and 1.97-1.90 Å for the Se-Met data sets.

[b]$R_{sym} = \sum|I - \langle I\rangle|/\sum I$, where I is the observed intensity and $\langle I\rangle$ is the average intensity from multiple observations of the symmetry related reflections.

[c]Phasing power is root mean square of $F_H/E$, where $F_H$ for anomalous and dispersive are $f$" and $f$' part of $F_H$, respectively, and $E$ is the lack-of-closure error.

## Supplementary methods

### Preliminary characterization of L-[$^3$H]-Leucine transport by $LeuT_{Aa}$ proteoliposomes

To determine the extent to which [$^3$H]-leucine transport depends upon membrane potential, uptake experiments were carried out in the presence and absence of valinomycin. $LeuT_{Aa}$ proteoliposomes were loaded with Buffer 1 (20 mM HEPES-Tris (pH 7.4), 100 mM potassium gluconate) and then divided into two aliquots. For the "minus valinomycin" condition, liposomes were used as prepared. For the "plus valinomycin" condition, these liposomes were preincubated with 1 μM valinomycin for 2 hours prior to use. Transport was initiated by adding the liposomes to Buffer 2 {20 mM HEPES-Tris, pH 7.4, 0.1 μM [$^3$H]-leucine (11.7 μCi/mL)} containing 100 mM NaCl either without or with 1 μM valinomycin, and the assays were carried out as described in the methods section of the main text. To gauge substrate specificity of $LeuT_{Aa}$, a competition experiment was performed. Proteoliposomes loaded with Buffer 1 supplemented with 1 μM valinomycin were added to Buffer 2 containing 100 mM NaCl,1 μM valinomycin, and either 100 μM L-leucine, 100 μM glycine, or 100 μM L-tryptophan. In each case, reactions were terminated after 4 min, and [$^3$H]-leucine uptake was normalized to that measured in the absence of a competitor.

**Supplementary Figure Legends**

**Figure S1** Stereoview of $LeuT_{Aa}$ from the cytoplasm. All settings are the same as in Fig. 2 in the main text.

**Figure S2** Dimer interface in the $LeuT_{Aa}$ crystal. **a**, The $LeuT_{Aa}$ dimer, as depicted in Fig. 3c. The black and gray boxes pinpoint those regions shown in panel b and c, respectively. **b** and **c**, Magnification of the dimer intermolecular interaction sites.

**Figure S3** Chloride ion binding site. Distances (Å) are written in bold letters. The chloride ion is represented as a magenta sphere, with all residues within 4 Å appearing as stick models.

**Figure S4** Preliminary characterization of [$^3$H]-leucine transport by $LeuT_{Aa}$ proteoliposomes. **a**, Effect of valinomycin. The closed circles and open squares represent uptake in the presence and absence of 1 μM valinomycin, respectively. The data points were fit to a single exponential (solid line). Error bars for each data point represent the standard deviation for triplicate measurements. **b**, Effect of competitors. Error bars for each data set represent the standard deviation for duplicate measurements.

**Figure S5** Water and aromatic residue distribution in $LeuT_{Aa}$. Leucine and detergent molecules are shown as stick models; the two sodium and single chloride ions are depicted as blue and magenta spheres, respectively. The approximate boundaries of the membrane bilayer are demarcated with horizontal lines in both a and c. **a**, Water molecules in the structure, with water

oxygen atoms represented as cyan spheres. **b**, Histogram of water molecule distribution as a function of membrane depth, divided into 5-Å bins along the crystallographic y-axis. **c**, Tryptophan and tyrosine residues in the structure. The 16 tryptophans and 17 tyrosines are shown as black stick models. The N$\varepsilon$1 nitrogen atoms in tryptophan and the hydroxyl oxygen atoms in tyrosine are displayed as navy and red spheres, respectively. **d**, Histogram of tryptophan and tyrosine distribution as a function of membrane depth, divided into 5-Å bins along the crystallographic y-axis. The navy and red bars indicate the number of tryptophan and tyrosine residues, respectively.

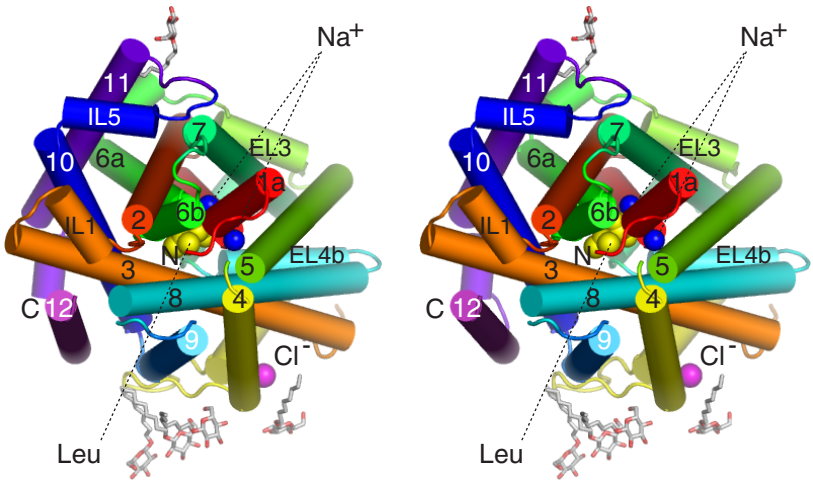


**Gouaux_Supplementary Fig S1**

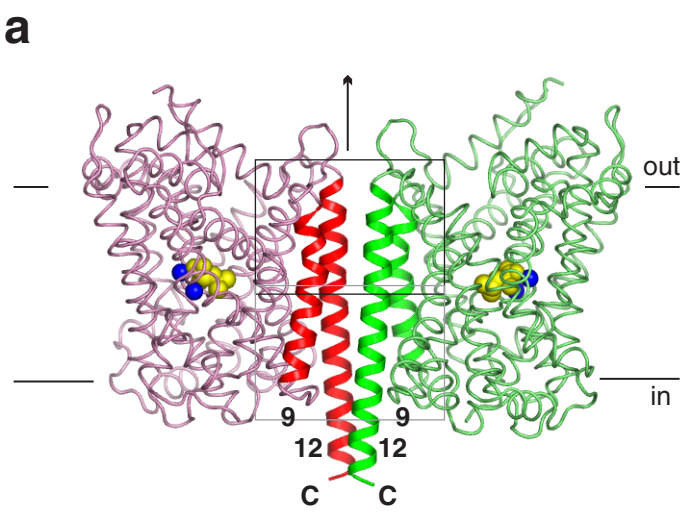


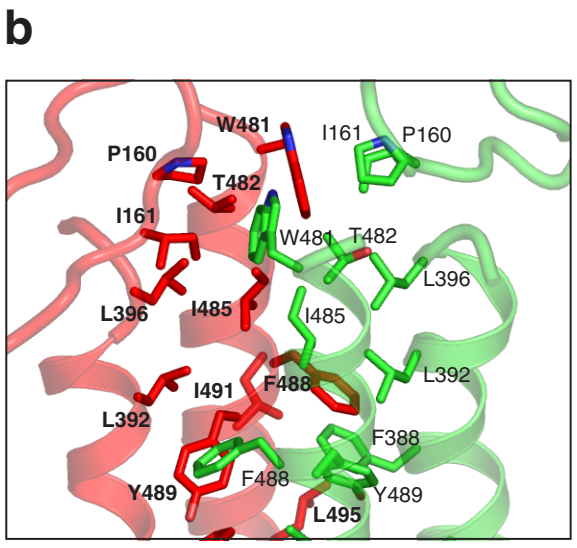


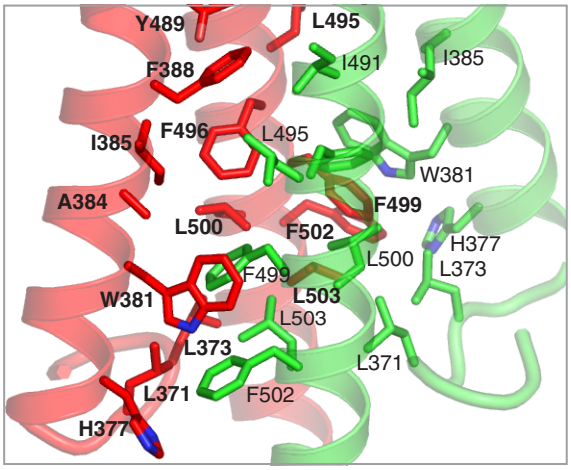


**Gouaux_Supplementary Fig S2**

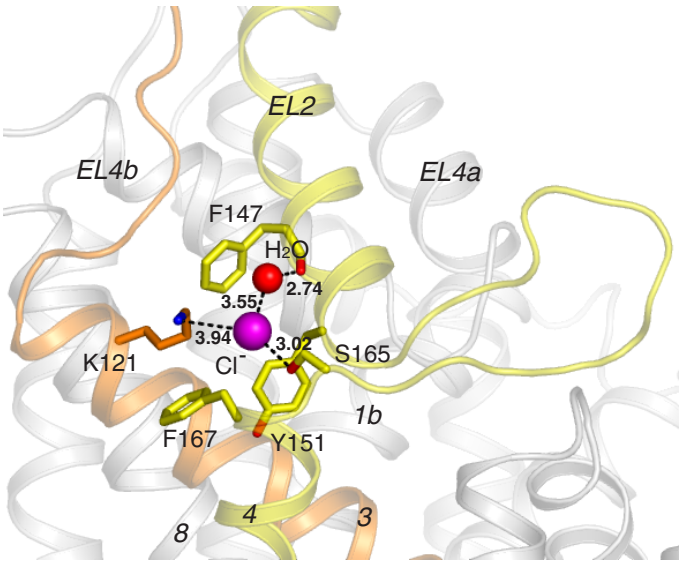


**Gouaux_Supplementary Fig S3**

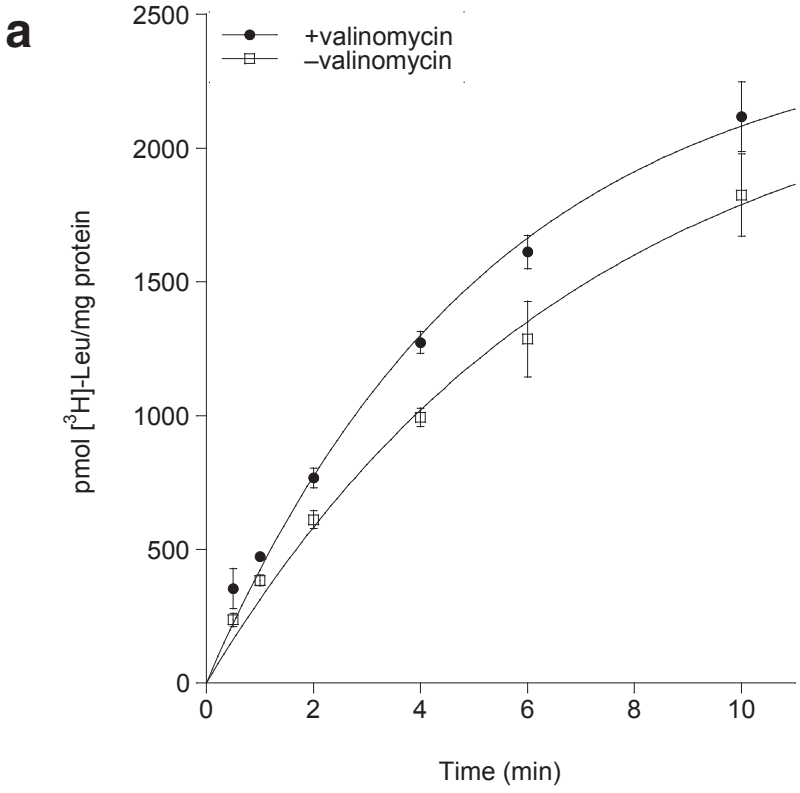


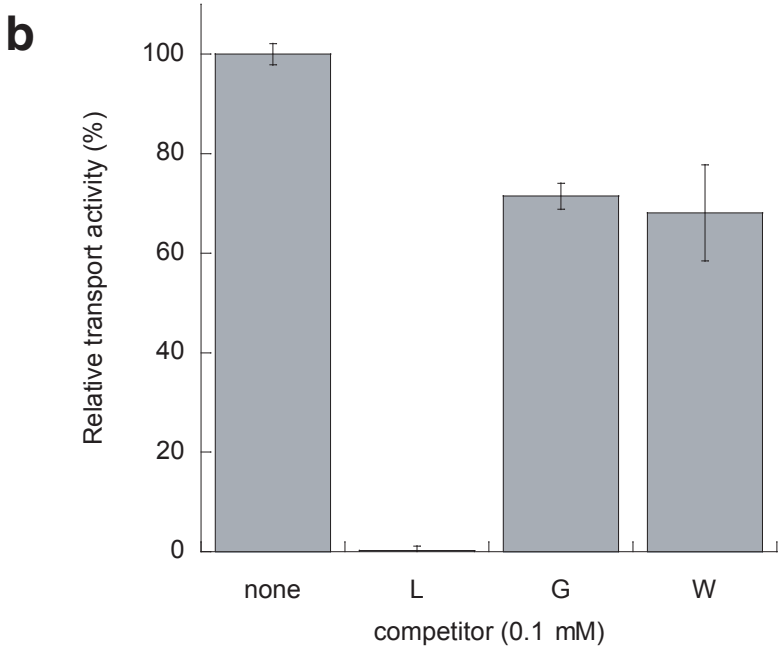


**Gouaux_Supplementary Fig S4**

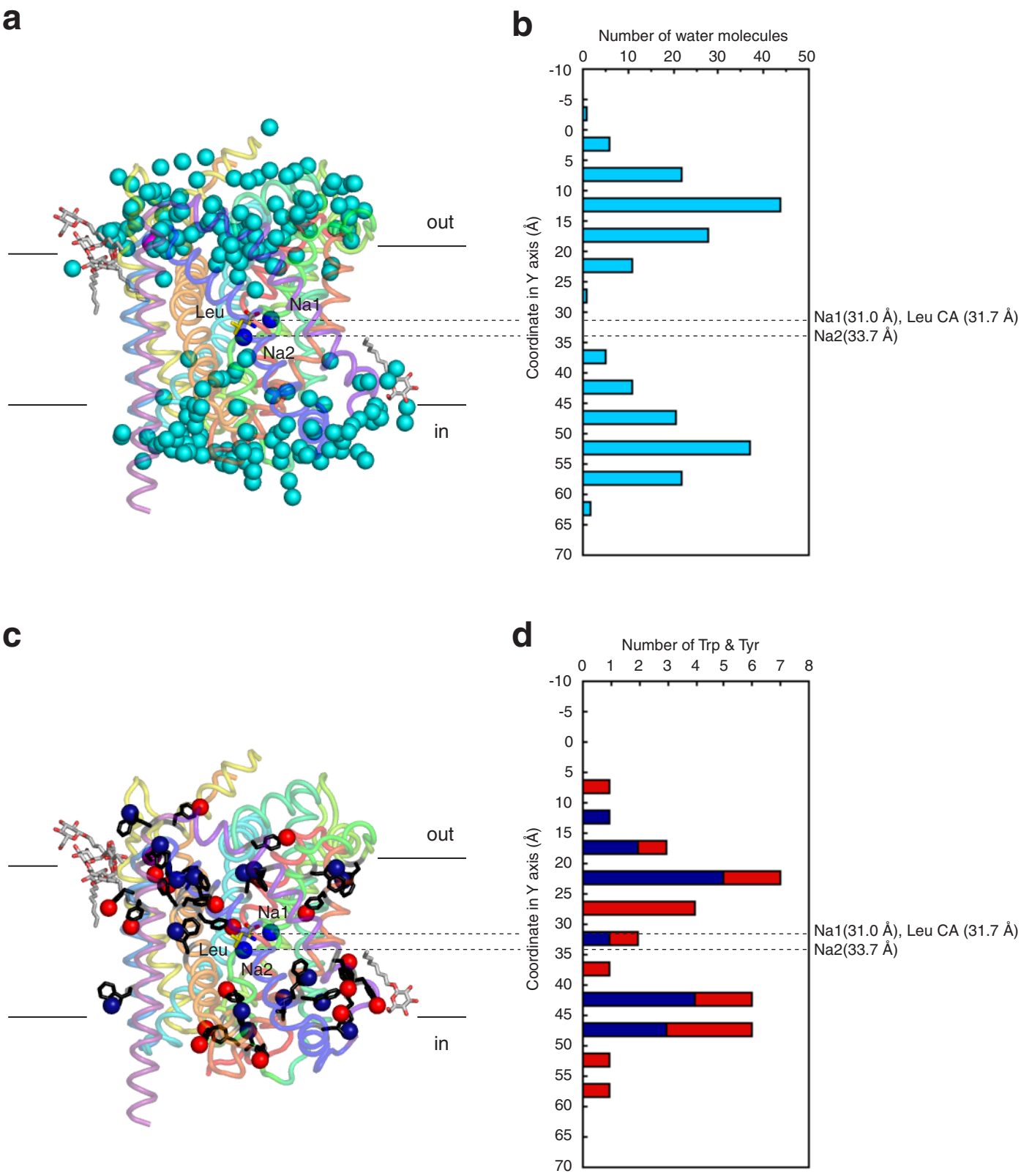


**Gouaux_Supplementary Fig S5**